Mar. Drugs **2011**, *9*, 1-x manuscripts; doi:10.3390/md90x000x

OPEN ACCESS

Marine Drugs

ISSN 1660-3397

www.mdpi.com/journal/marinedrugs

Article

Bioactive Cembranoids from the Soft Coral *Sinularia crassa*

Chih-Hua Chao [1,2], Kuei-Ju Chou [1], Chiung-Yao Huang [1], Zhi-Hong Wen [1,3], Chi-Hsin Hsu [1,3], Yang-Chang Wu [4], Chang-Feng Dai [5], and Jyh-Horng Sheu [1,3,*]

[1] Department of Marine Biotechnology and Resources, National Sun Yat-Sen University, Kaohsiung 804, Taiwan; E-Mails: chaochihhua@hotmail.com (C.-H.C.); jzusmile@hotmail.com (K.-J.C.); betty8575@yahoo.com.tw (C.-Y.H.)

[2] Chinese Medicinal Research and Development Center, China Medical University and Hospital, Taichung 404, Taiwan, ROC

[3] Asian Pacific Ocean Research Center, National Sun Yat-sen University, Kaohsiung 804, Taiwan E-Mails: wzh@mail.nsysu.edu.tw (Z.-H.W.); hsuch@mail.nsysu.edu.tw (C.-H.H.)

[4] College of Chinese Medicine, China Medical University, Taichung 404, Taiwan E-Mail: yachwu@mail.cmu.edu.tw (Y.-C.W.)

[5] Institute of Oceanography, National Taiwan University, Taipei, Taiwan; E-Mail: corallab@ntu.edu.tw (C.-F.D.)

* Author to whom correspondence should be addressed; E-mail: sheu@mail.nsysu.edu.tw (J.-H.S.)

Received: / Accepted: / Published:

Abstract: Eight new cembranoids, crassarines A–H (**1**–**8**) were isolated from a Formosan soft coral *Sinularia crassa*. Compounds **1**–**3** represent the rare cembranoids with a 1,12-oxa-bridged tetrahydrofuran ring, while **4** and **5** are the firstly discovered 1,11-oxa-bridged tetrahydropyranocembranoids. The absolute configuration of **6** was determined using the Mosher's method. Compounds **6** and **8** were found to significantly inhibit the expression of both pro-inflammatory iNOS and COX-2 proteins at 10 μM, respectively, while compounds were found to be non-cytotoxic toward the selected human liver cancer cells.

Keywords: *Sinularia crassa*; crassarines A–H; anti-inflammatory

1. Introduction

Soft corals were proven to be a rich source of terpenoids [1]. We previously have isolated a series of bioactive cembrane- [2–4] and norcembrane- [5–8] diterpenoids from the Formosan soft corals of the genus *Sinularia*. Although this genus has been well studied regarding bioactive constituents, previous investigations on an Indian soft coral *Sinularia crassa* (Tixier-Durivault, 1951) had resulted in the isolation of only a sphingosine and a steroid possessing anti-inflammatory [9,10] and 5α-reductase inhibitiory activities [11], respectively. This prompted us to investigate the bioactive compounds from the Formosan soft coral *S. crassa* and the present study has led to the isolation of eight new cembranoids, crassarines A–H (**1**–**8**, see Chart 1) from the ethanolic extract of this organism. The structures of these compounds have been established by extensive spectroscopic analysis and chemical method. The anti-inflammatory activity of **1**–**8** to inhibit up-regulation of the pro- inflammatory iNOS (inducible nitric oxide synthase) and COX-2 (cyclooxygenase-2) proteins in LPS (lipopolysaccharide)-stimulated RAW264.7 macrophage cells and the cytotoxicity of compounds **4**–**8** against a panel of cancer cell lines including human liver carcinoma (HepG2 and HepG3), human breast carcinoma (MCF-7 and MDA-MB-231), and human lung carcinoma (A-549) were evaluated in order to discover bioactive natural products.

Chart 1. The structures of crassarines A–H (**1**–**8**).

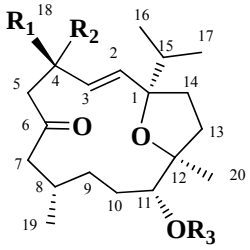

1 $R_1 = CH_3$, $R_2 = OH$, $R_3 = H$
1a $R_1 = CH_3$, $R_2 = OH$, $R_3 = Ac$
2 $R_1 = OH$, $R_2 = CH_3$, $R_3 = Ac$
3 $R_1 = OH$, $R_2 = CH_3$, $R_3 = CHO$

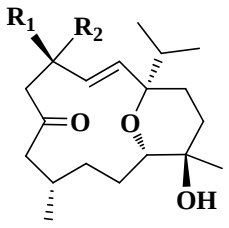

4 $R_1 = OH$, $R_2 = CH_3$
5 $R1 = CH_3$, $R_2 =$ OH

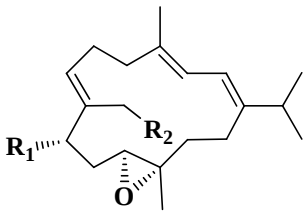

6 $R_1 = OH$, $R_2 = H$
7 $R_1 = H$, $R_2 = OH$

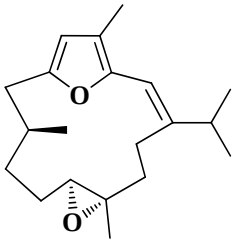

8

2. Results and Discussion

The ethanolic extract of the soft coral *S. crassa* was partitioned between EtOAc and H_2O to afford the EtOAc-soluble fraction, which was subjected to silica gel column chromatography. The fractions containing terpenoids were selected based on characteristic peaks of methyl groups in the ^1H NMR spectrum. These fractions were subsequently subjected to a series of chromatographic separations to afford pure compounds **1**–**8**.

The HRESIMS of crassarine A (**1**) exhibited a pseudomolecular ion peak at *m/z* 361.2353 $[M+Na]^+$, consistent with a molecular formula of $C_{20}H_{34}O_4$, appropriate for four degrees of unsaturation. The IR spectrum of **1** showed a broad absorption band at 3461 cm^{-1} and a strong absorption band at 1698 cm^{-1}, implying the presence of hydroxy and carbonyl groups. The latter was identified as a ketone functionality from the carbon resonance at δ 211.8 (Table 1). In addition, carbon resonances at δ 133.3 (CH) and 134.3 (CH) were attributed to the presence of an 1,2-disubstituted double bond. The above functionalities accounted for two of the four degrees of unsaturation, suggesting a bicyclic structure in **1**. By interpretation of ^1H–^1H COSY correlations, it was possible to establish three partial structures from both H-7 and H_3-19 to H-8, H-8 to H-11, H_2-13 to H_2-14, and both H_3-16 and H_3-17 to H-15.

Subsequently, these partial structures were connected by the HMBC correlations (Figure 1). According to the downfield-shifted carbon chemical shifts at δ 88.1 (C-1, C), 75.0 (C-11, CH), and 85.7 (C-12, C) [12] as well as the HMBC correlations from H_3-20 to C-11, C-12, and C-13 and H_3-16 (or H_3-17) to C-17 (or C-16), C-15, and C-1, an ether linkage between C-1 and C-12 forming a tetrahydrofuran (THF) ring and a hydroxy group at C-11 were assigned for **1**. The location of C-6 ketone was suggested from the carbon resonances of the adjacent methylenes at δ 53.3 (C-5) and 51.6 (C-7). This was further confirmed by the HMBC correlations from both H_2-7 and H_2-5 to C-6. In addition, the HMBC correlations from H_3-18 to C-3, C-4, and C-5 helped to locate the C-2/C-3 double bond and a hydroxy group at quaternary C-4 (δ 71.4). Hence, the planar structure of **1**, a cembranoid possessing a 1,12-bridged tetrahydrofuran ring, was established as shown in Figure 1.

Table 1. ^{13}C NMR spectroscopic data of compounds **1**–**8**

#	**1**[a]	**1**[b]	**2**[c]	**3**[a]	**4**[a]	**5**[a]	**6**[d]	**7**[d]	**8**[d]
1	88.1	87.6	88.6	88.8	77.5	77.7	147.2	147.7	146.2
2	133.3	133.8	133.4	133.2	131.6	130.8	119.1	118.6	107.7
3	134.3	135.1	136.4	136.5	139.0	138.3	121.7	122.9	146.8
4	71.4	70.7	72.4	72.4	73.4	71.7	135.4	134.8	117.0
5	53.3	56.4	52.7	52.7	54.0	50.8	38.5	39.4	109.6
6	211.8	209.5	212.9	213.0	215.2	215.7	25.2	25.5	151.1
7	51.6	49.4	51.1	51.2	53.1	54.2	126.7	130.1	35.3
8	28.9	25.8	26.4	26.4	30.8	28.5	136.7	138.0	30.4
9	32.5	32.7	32.9	33.0	32.4	29.7	75.3	33.7	30.2
10	29.4	26.5	26.8	26.9	26.0	24.4	32.3	25.5	24.8
11	75.0	71.1	77.0	77.0	76.2	74.7	57.0	59.1	65.4
12	85.7	86.4	84.7	84.7	70.0	70.1	59.5	60.3	60.7
13	35.2	36.7	34.6	34.4	37.1	36.9	36.4	35.4	40.5
14	30.9	30.4	31.7	31.9	28.4	28.8	24.3	24.1	24.2
15	37.7	38.0	38.6	38.5	40.2	40.3	34.4	33.5	35.2
16	18.0	18.3	18.2	18.2	17.3	17.2	22.5	22.3	21.6
17	17.7	17.8	17.6	17.5	16.8	16.8	22.3	22.7	21.1
18	28.9	31.1	29.8	29.7	28.9	24.5	17.3	16.8	9.1
19	22.6	22.1	22.3	22.3	22.0	20.7	11.7	59.4	20.0
20	23.4	20.8	23.5	24.0	18.8	19.5	18.5	19.0	15.2
OAc			170.9						
			21.0						
CHO				160.9					

[a] Spectra were measured in $CDCl_3$ (100 MHz). [b] Spectra were measured in pyridine-d_5 (100 MHz). [c] Spectra were measured in $CDCl_3$ (125 MHz). [d] Spectra were measured in C_6D_6 (100 MHz).

Table 2. ^{1}H NMR Spectroscopic Data of Compounds **1**–**3** and **8**.

#	**1**, δ_H (*J* in Hz) [a]	**1**, δ_H (*J* in Hz) [b]	**2**, δ_H (*J* in Hz) [c]	**3**, δ_H (*J* in Hz) [a]	**8**, δ_H (*J* in Hz) [d]
2	5.73, s	6.28, d (16.0)	5.75, s	5.74, s	5.95, s
3	5.73, s	6.04, d (16.0)	5.75, s	5.74, s	
5	a: 2.79, d (15.6)	a: 2.98, d (13.0)	a: 2.89, d (15.0)	a: 2.89, d (15.0)	5.73,s
	b: 2.61, d (15.6)	b: 2.87, d (13.0)	b: 2.48, d (15.0)	b: 2.48, d (15.0)	
7	a: 2.45, dd (15.6, 8.4)	a: 3.38, dd (16.0, 4.0)	a: 2.52, dd (18.0, 8.5)	a: 2.49, dd (18.0, 8.5)	a: 2.44, br d (12.4)
	b: 2.23, dd (15.6, 5.2)	b: 2.04, dd (16.0, 9.6)	b: 2.16, dd (18.0, 4.0)	b: 2.18, dd (18.0, 4.0)	b: 2.02, m
8	2.02, m	2.41, m	2.29, m	2.29, m	1.96, m
9	1.46, m	1.30, m	1.37, m	1.38, m	1.30, m
			0.97, m	0.99, m	0.93, m
10	a: 1.56, m	a: 2.18, m	a: 1.44, m	a: 1.48, m	a: 1.82, m
	b: 1.25, m	b: 1.63, m	b: 1.38, m	b: 1.37, m	b: 1.20, m
11	3.24, br d (9.6)	3.76, d (10.4)	4.80, br d (10.5)	4.90, br d (8.4)	2.36, dd (10.0, 2.0)
13	a: 1.98, m	a: 2.61, ddd (12.4, 8.4, 2.4)	a: 1.80, m	a: 1.84, m	a: 2.40, m
	b: 1.68, m	b: 1.75, m	b: 1.60, m	b: 1.64, m	b: 1.04, m
14	a: 1.96, m	a: 2.12, m	a: 1.98, m	a: 2.01, m	a: 3.55, dd (12.4, 9.2)
	b: 1.89, m	b: 1.88, m	b: 1.87, m	b: 1.86, m	b: 2.02, m
15	1.76, m	1.81, m	1.75, m	1.75, m	2.22, m
16	0.87, d (6.8)	0.92, d (6.8)	0.86, d (6.8)	0.86, d (6.8)	1.00, d (6.0)
17	0.86, d (6.8)	0.92, d (6.8)	0.84, d (6.8)	0.84, d (6.8)	1.04, d (6.0)
18	1.37, s	1.61, s	1.25, s	1.25, s	1.88, s
19	0.98, d (6.4)	0.94, d (6.8)	0.91, d (6.4)	0.92, d (6.8)	0.82, d (6.4)
20	1.25, s	1.49, s	1.15, s	1.18, s	1.23, s
OAc			2.09,s		
OCH				8.18,s	
4-OH			4.45, s	4.47, s	

[a] Spectra were measured in $CDCl_3$ (400 MHz). [b] Spectra were measured in pyridine-d_5 (400 MHz). [c] Spectra were measured in $CDCl_3$ (500 MHz). [d] Spectra were measured in C_6D_6 (400 MHz).

The *E* geometry for the C-2/C-3 double bond was deduced. from a 16.0 Hz coupling constant (Table 1) between H-2 and H-3. The relative configuration of **1** was determined by the interpretation of NOE correlations (Figure 2). The NOE correlations between H_3-20/H_3-16 (or H_3-17), H-11/H-13a (δ_H 2.61), H-11/H-8, and H_3-20/H_2-13 suggested the 1*S**,8*S**,11*R**,12*S** configuration as depicted in Figure 2. In addition, the NOE correlations observed for H-2 with both H-15 and H_3-18 and for H_3-18 with H-3 suggested the 4*S** configuration. In order to understand the orientation of 4-OH and 11-OH, the pyridine-induced solvent shifts were measured [13,14]. The significant differences of chemical shifts

($\Delta\delta = \delta CDCl_3 - \delta C_5D_5N$) due to pyridine-induced deshielding effect of hydroxy group were observed for H-7a ($\Delta\delta$ = – 0.93 ppm), H_3-20 ($\Delta\delta$ = – 0.24 ppm), and H-13a ($\Delta\delta$ = – 0.63 ppm) (Table 2), suggesting that 4-OH is close to H-7a, and the 11-OH is not only close to H-13a but also gauche-oriented to H_3-20, as shown in Figure 2. To determine the absolute configuration, we applied the Mosher's method on **1**. However, we were unable to prepare the corresponding Mosher esters of **1** by usual reaction conditions [3,4]. This might be due to the steric hindrance of THF ring adjacent to C-11.

Figure 1. Selected ^1H–^1H COSY (▬) and HMBC (→) correlations of **1**–**8**.

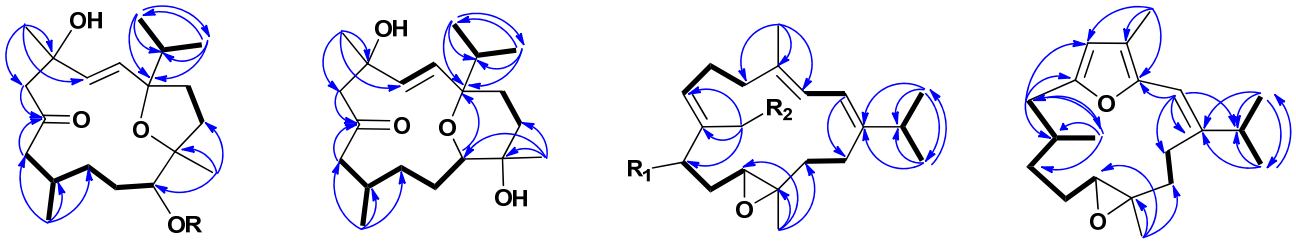

HRESIMS analysis of crassarine B (**2**) provided a molecular formula of $C_{22}H_{36}O_5$ ($[M+Na]^+$ *m/z* 403.2463). The ^1H and ^{13}C NMR spectroscopic data of **2** were close to those of **1**. A comparison of NMR spectroscopic data of **2** with those of **1** indicated that **2** possesses an acetoxy group [δ_C 170.9 (C), δ_C 21.0 (CH_3); δ_H 2.09], which was suggested to be attached at C-11 due to the downfield-shifted proton resonance at δ_H 4.08 (1H, br d, J = 10.5 Hz, H-11) in comparison with the relevant case of 11-OH analogue **1** (δ_H 3.24, 1H, br d, J = 9.6 Hz, H-11). The structure elucidation of **2** was accomplished by an extensive analysis of its 2D NMR correlations, which led to the establishment of its planar structure, as shown in Figure 1. Except for the C-11 substituent and the THF ring in both compounds **1** and **2**, the differences were observed for the chemical shifts of protons and carbons around the C-4 asymmetric center, in particular those of H_3-18 (δ_H 1.37 and δ_C 28.9 for **1**; δ_H 1.25 and δ_C 29.8 for **2**). These observations suggested that the configuration at C-4 in **2** should be opposite to that in **1**. Moreover, **1** and **2** shared the same NOE correlations around asymmetric centers C-1, C-8, C-11, and C-12. To confirm the above elucidation, **1** was acetylated to obtain **1a**, which displayed different ^1H NMR spectrum to that of **2** (see Experimental). Consequently, **2** was determined to be the 4-*epi*-11-*O*-acetyl derivative of **1**. The ^{13}C and ^1H NMR spectral data of **3** are very similar to that of **2** (Tables 1 and 2); however, ^1H NMR spectrum of **3** showed a singlet at δ 8.18 which correlates with carbon signal at δ 160.9 in the HSQC spectrum, indicating the presence of a formyloxy group at C-11 in **3**. On the basis of the above data, **3** was identified as the 11-O-formyl derivative of **2**. Literature review showed that this is the first cembranoid with a formyloxy functionality.

Crassarine D (**4**) possesses the same molecular formula as that of **1**. The ^{13}C NMR data (Table 1) of **4** were mostly similar to those of **1**, except for those of sp^3 oxygenated carbons, suggesting that they vary mainly in heterocyclic ring. The upfield shift for H-11 from δ 3.24 (1H, br d, J = 9.6 Hz) in **1** to δ 3.02 (1H, d, J = 8.8 Hz) in **4** indicates that an ether linkage should be located between C-1 and C-11 to form a tetrahydropyran (THP) ring. The HMBC correlation from H-11 to C-1 (δ 77.5, C) confirmed the presence of this THP ring in **4**, rather than the THF ring in **1**. The detailed analysis of the

correlations observed in the COSY, HMBC, and HSQC spectra further assigned all the spectroscopic data and established the planar structure of **4** (Figure 1). The *E* geometry of C-2/C-3 double bond was also deduced from the coupling constant (16.0 Hz) between H-2 and H-3. NOE correlations between H_3-20/H-14a, H_3-17/H-14a, H_3-20/H-13a, and H-11/H-13b suggested that H-11 is an axial proton and oriented oppositely to H_3-20. Both H-11 and H-8 were suggested to be positioned on the same face based on the observation of NOE correlations between H-11/H-8, H-8/H-10a, and H-10a/H-11. In addition, H-3 showed NOE correlations with both H_3-18 and H-15 (Figure 2), revealing that H_3-18 should be pointed toward the same orientation as that of the isopropyl group. Consequently, the 1*S**,4*R**,8*S**,11*S**,12*R** configuration was suggested for **4**.

Figure 2. Selected NOE correlations for compounds **1**, **4**, **6**, and **8**.

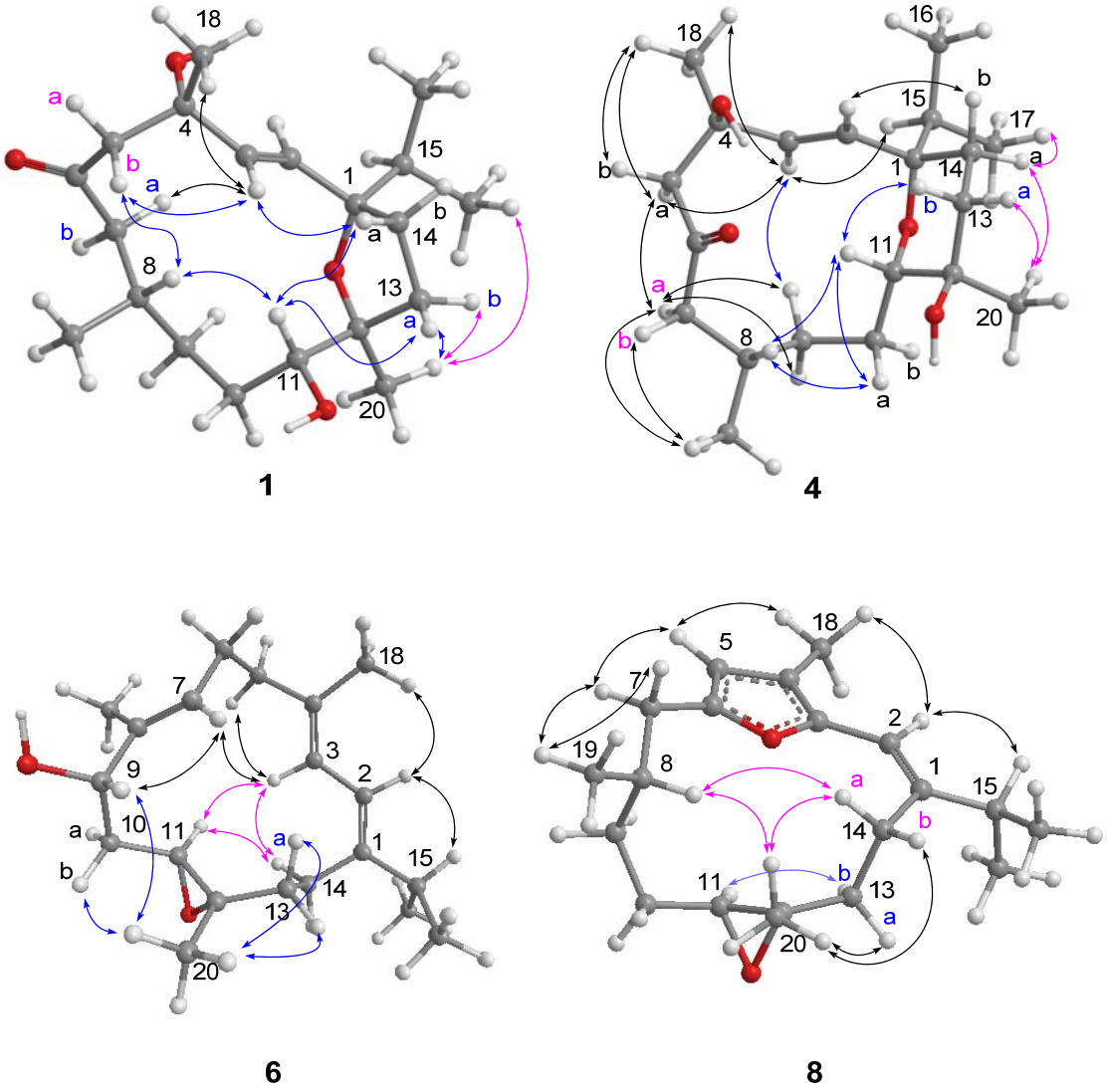

Table 3. ^{1}H NMR Spectroscopic Data of Compounds **4**–**7**.

#	**4**[a], δ_H (*J* in Hz)	**5**[a], δ_H (*J* in Hz)	**6**[b], δ_H (*J* in Hz)	**7**[b], δ_H (*J* in Hz)
2	5.81, d (16.0)	5.58, d (16.0)	6.06, d (10.4)	6.08, d (10.8)
3	5.89, d (16.0)	6.07, d (16.0)	5.90, dd (10.4, 1.2)	6.02, d (10.8)
5	a: 2.80, d (16.0)	a: 3.01, d (16.6)	2.04, m	2.00, m
	b: 2.72, d (16.0)	b: 2.41, d (16.6)		
7	a: 2.39, dd (13.6, 11.2)	a: 2.46, dd (11.6, 2.8)	2.10, m	a: 2.13, m
	b: 2.16, dd (13.6, 2.4)	b: 2.07, dd (12.0, 11.6)		b: 2.00, m
8	1.92, m	1.96, m	5.50, dd (7.2, 6.0)	5.26, dd (9.2, 5.2)
9	a: 1.32, m	a: 1.56, m	4.00, dd (8.0, 3.2)	a: 2.36, m
	b: 1.18, m	b: 0.99, m		b: 2.29, m
10	a: 1.49, m	a: 1.57, m	a: 1.99, m	a: 1.72, m
	b: 1.19, m	b: 1.26, m	b: 1.67, m	b: 1.64, m
11	3.02, d (8.8)	3.19, d (10.4)	2.87, dd (7.6, 6.0)	3.00, dd (6.8, 5.2)
13	a: 1.74, m	a: 1.72, m	a: 1.85, m	a: 1.91, m
	b: 1.57, m	b: 1.51, m	b: 1.52, m	b: 1.62, m
14	a: 1.68, m	a: 1.65, m	a: 2.23, m	a: 2.40, m
	b: 1.59, m	b: 1.59, m	b: 1.92, m	b: 1.90, m
15	1.77, m	1.80, m	2.16, m	2.21, m
16	0.78, d (6.8)	0.80, d (7.0)	0.99, d (6.8)	1.00, d (6.8)
17	0.91, d (6.8)	0.90, d (7.0)	0.99, d (6.8)	0.99, d (6.8)
18	1.37, s	1.38, s	1.65, s	1.63, s
19	0.98, d (6.4)	1.00, d (6.4)	1.40, s	3.93, d (12.0)
				3.89, d (12.0)
20	1.11, s	1.15, s	1.12, s	1.15, s

[a] Spectra were measured in $CDCl_3$ (400 MHz). [b] Spectra were measured in C_6D_6 (400 MHz).

Crassarine E (**5**) has the same molecular formula as that of **4**. The ^{1}H and ^{13}C NMR spectroscopic data as well as the proton coupling patterns of **5** are similar to those of **4**. A comparison of NMR spectroscopic data of **5** with those of **4** showed some differences in chemical shifts for protons and carbons neighboring C-4 and C-8, suggesting that they are epimeric at either C-4 or C-8. The NOE correlation between H_3-18 and H-2 in **5**, instead of H_3-18 and H-3 in **4** (Figure 2) suggested that compound **5** is a 4-epimer of **4**.

Crassarine F (**6**) was assigned a molecular formula of $C_{20}H_{32}O_2$, according to the HRESIMS and NMR spectroscopic data (Tables 1 and 3). The IR absorption band at 3300 cm^{-1} revealed the presence of hydroxy group. A tetrasubstituted 1,3-butadiene [δ_H 6.06 (1H, d, J = 10.4 Hz) and 5.90 (1H, dd, J = 10.4, 1.2 Hz); δ_C 147.2 (C), 135.4 (C), 121.7 (CH), and 119.1 (CH)] , a trisubstituted double bond [δ_H 5.50 (1H, dd, J = 7.2, 6.0 Hz); δ_C 136.7 (C), and 126.7 (CH)], and a trisubstituted epoxide [δ_H 2.87 (1H, dd, J = 7.6, 6.0 Hz); δ_C 59.5 (C) and 57.0 (CH)] were also evident. Above NMR signals suggested **6** to be the 1,3-diene cembranoid with an epoxy functionality [15]. The 11,12-epoxy group was assigned by the HMBC correlations from H_3-20 to C-11, C-12, and C-13 and H_2-14 to C-1, C-2, and C-13 (Figure 1). The COSY cross peaks of H_2-10/H-11 and H_2-10/H-9 as well as the HMBC correlations from H_3-

19 to C-7, C-8, and C-9 assigned the hydroxy group at C-9 (δ_C 75.3, CH). These findings and the detailed COSY and HMBC correlations established the planar structure of **6**, as shown in Figure 1. The relative configuration of **6** was determined by the interpretation of NOESY spectrum. The crucial NOE correlations (Figure 2) between H-2/H_3-18, H-2/H-15, and H-9/H-7 indicated the E geometry for all double bonds and suggested a s-*trans* geometry for the 1,3-diene. NOE correlations between H-11/H-3, H-11/H-14a, and H-3/H-14a showed that these protons should be pointed toward the core of 14-membered ring. Furthermore, the absence of NOE correlation between H-11 and H_3-20 and the presence of correlation between H-9 and H_3-20 suggested the 9*S**,11*S**,12*S** configuration, as depicted in Figure 2. The absolute configuration of **6** was determined by the application of Mosher's method [16,17]. The (*S*)- and (*R*)-MTPA esters of **6** (**6a** and **6b**, respectively) were prepared using the corresponding (*R*)- and (*S*)-MTPA chloride, respectively. The determination of chemical shift differences for the protons neighboring C-9 led to the assignment of the 9*S* configuration in **6** (Figure 3). Thus, the absolute configuration of **6** was determined as 9*S*, 11*S*, 12*S*.

Figure 3. ^{1}H NMR chemical shift differences of MTPA esters of **6**.

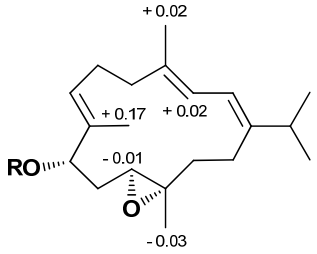

$\triangle\delta = \delta\,(S) - \delta\,(R)$ MTPA ester

6a R = (*S*)-MTPA
6b R = (*R*)-MTPA

The HRESIMS data of crassarine G (**7**) revealed a molecular formula of $C_{20}H_{32}O_2$, the same as that of **6**. The IR spectrum of **7** disclosed the presence of hydroxy group (ν_{max} 3434 cm^{-1}). A comparison of the NMR spectroscopic data of **7** (Tables 1 and 2) with those of **6** revealed that the hydroxy-containing methine (C-9) in **6** was replaced by a sp^3 methylene in **7**. It was also found that resonances appropriate for H_3-19 in **6** were absent from the ^{1}H and ^{13}C NMR spectra of **7** and replaced by signals for a hydroxymethyl group [δ_H 3.93 and 3.89 (each 1H, d, J = 12.0 Hz); δ_C 59.4 (CH_2)]. Careful inspection of the 2D NMR spectra of **7** confirmed the above elucidation.

The HRESIMS and ^{13}C NMR spectroscopic data of crassarine H (**8**) established a molecular formula of $C_{20}H_{30}O_2$ and six degrees of unsaturation. The ^{13}C NMR spectrum showed the presence of a trisubstituted double bond [δ_C 146.2 (C) and 107.7 (CH)] and a trisubstituted epoxide [δ_C 65.4 (CH) and 60.7 (C)]. In addition, the carbon resonances at δ_C 9.1 (CH_3, C-18), 151.1 (C, C-6), 146.8 (C, C-3), 109.6 (CH, C-5), and 117.0 (C, C-4) are attributed to the presence of a 2,5-dialkyl-3-methylfuran [18]. This furan moiety and the trisubstituted double bond were found to be conjugated according to the downfield-shifted proton resonance of H-2 at δ 5.95 (1H, s) [18]. This was further confirmed by the HMBC correlations from H-2 to C-1, C-3, C-14, and C-15, H_3-18 to C-3, C-4, and C-5, and H-5 to C-3,

C-4, and C-6. The above data together with the detailed inspection of the COSY and HMBC correlations of **8** established its planar structure (Figure 1). The relative configuration of **8** was determined mainly by the assistance of the NOESY experiment. The key NOE correlations between H-2 and both H-15 and H_3-18 indicated an *E* geometry of C-1/C-2 double bond (Figure 2). The *trans* epoxy group was deduced by the NOE correlations between H-11/H-13b and H_3-20/H-13a. In addition, H-8 showed an NOE correlation with H_3-20, instead of H-11, suggesting the 8*S**,11*S**,12*S** configuration for **8**.

Figure 4. Effect of compounds **1**–**8** at 10 μM on the LPS-induced pro-inflammatory iNOS and on COX-2 protein expression of RAW264.7 macrophage cells by immunoblot analysis (A) Immunoblots of iNOS and β-actin. (B) Immunoblots of COX-2 and β-actin. The values are means ± SEM (n = 6). The relative intensity of the LPS alone stimulated group was taken as 100%. *Significantly different from LPS alone stimulated group (*P < 0.05). [a]Stimulated with LPS. [b]Stimulated with LPS in the presence of **1**–**8** (10 μM).

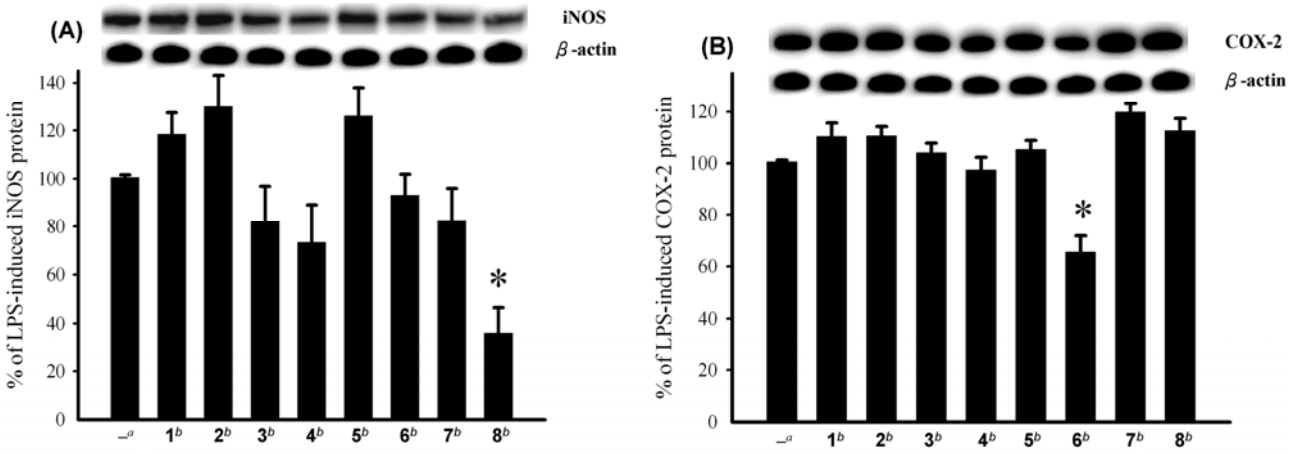

The anti-inflammatory activity of diterpenoids **1**–**8** against the accumulation of pro-inflammatory iNOS and COX-2 proteins in RAW264.7 macrophage cells stimulated with LPS was evaluated using immunoblot analysis. At a concentration of 10 μM (Figure 4), **8** was found to significantly reduce the levels of iNOS protein (35.8 ± 10.7%), compared with the control cells stimulated with LPS only. At the same concentration, **6** could reduce COX-2 expression (65.6 ± 6.2%) by LPS treatment. Cytotoxicity of diterpenoids **4**–**8** against HepG2, HepG3, MCF-7, MDA-MB-231, and A-549 cancer cell lines was also evaluated. The results showed that the tested compounds were found to be inactive toward the above cancer cell lines.

3. Experimental Section

3.1. General Experimental Procedures

The melting point was determined using a Fisher-Johns melting point apparatus. Optical rotations were determined with a JASCO P1020 digital polarimeter. IR spectrum was obtained on a JASCO FT/IR-4100 spectrophotometer. The NMR spectra were recorded on a Bruker AVANCE 300 FT-NMR

(or Varian 400 MR NMR/Varian Unity INOVA 500 FT-NMR) instrument at 300 MHz (or 400/500 MHz) for ^{1}H (referenced to TMS, δ_H 0.00 ppm, for both $CDCl_3$ and C_5D_5N and 7.15 ppm for C_6D_6) and 75 MHz (or 100/125 MHz) for ^{13}C (referenced to δ_C 77.0 for $CDCl_3$, to 128.0 ppm for C_6D_6, and to internal TMS at δ_C 0.0 ppm for C_5D_5N). ESIMS were recorded by ESI FT-MS on a Bruker APEX II mass spectrometer. Silica gel 60 (Merck, 230–400 mesh) and LiChroprep RP-18 (Merck, 40–63 μm) were used for column chromatography. Precoated silica gel plates (Merck, Kieselgel 60 F254, 0.25 mm) and precoated RP-18 F254S plates (Merck, 1.05560) were used for TLC analyses. High-performance liquid chromatography (HPLC) was performed on a Hitachi L-7100 pump equipped with a Hitachi L-7400 UV detector at 210 nm and a semi-preparative reversed-phase column (Merck, Hibar Purospher RP-18e, 5 μm, 250 × 10 mm).

3.2. Animal Material

The soft coral *Sinularia crassa* was collected by hand using scuba off the coast of Sansiantai, Taitung county, in July 2008, at a depth of 10 m, and was stored in a freezer. This soft coral was identified by one of the authors (C.-F. D.). A voucher specimen (specimen no. SST-03) was deposited in the Department of Marine Biotechnology and Resources, National Sun Yat-sen University.

3.3. Extraction and Isolation

The frozen bodies of *S. crassa* (1.1 kg fresh wt) were minced and extracted exhaustively with EtOH (3 × 2 L). The organic extract was concentrated to an aqueous suspension and was further partitioned between EtOAc and H_2O. The EtOAc extract (17.0 g) was fractionated by open column chromatography on silica gel using *n*-hexane–EtOAc and EtOAc–MeOH mixtures of increasing polarity to yield 32 fractions. Fraction 19, eluting with *n*-hexane–EtOAc (5:1), was further separated by silica gel column chromatography with gradient elution (*n*-hexane–EtOAc, 24:1 to 0:1) and followed by RP-18 open column (MeOH–H_2O, 50 % to 100%) to yield three subfractions (19A–19C). Subfraction 19A was subjected to RP-18 HPLC (MeOH–H_2O, 90%) to obtain compound **8** (2.2 mg). Similarly, compounds **2** (1.1 mg) and **3** (1.0 mg) were obtained from subfraction 19C using RP-18 HPLC (MeOH–H_2O, 75%). Subfraction 19B was fractionated over silica gel using gradient elution (*n*-hexane–EtOAc, 24:1 to 0:1) to yield three subfractions (19B-1–19B-3). Compounds **4** (3.4 mg) and **5** (2.3 mg) were obtained from subfractions 19B-1 and 19B-2, respectively, using RP-18 HPLC (MeOH–H_2O, 66%). Subfraction 19B-3 was subjected to normal phase HPLC (*n*-hexane–EtOAc, 2:1) to obtain **1** (2.3 mg). Fractions 22 to 24, eluting with *n*-hexane–EtOAc (1:1), were combined and further separated over silica gel column chromatography (*n*-hexane–EtOAc, gradient elution, 18:1 to 0:1) to give a residue containing terpenoids. This residue was separated over RP-18 column chromatography using gradient elution (MeOH–H_2O, 50% to 100%) to obtain two subfractions (23A and 23B). Subfraction 23A was further purified by RP-18 HPLC (MeOH–H_2O, 75%) to yield compound **6** (1.8 mg). In the same manner, compound **7** (8.7 mg) was obtained from subfraction 23B using RP-18 HPLC (MeOH–H_2O, 80%).

Crassarine A (**1**): colorless oil; $[\alpha]^{24}_{D}$ –93(c 0.20, $CHCl_3$); IR (KBr) ν_{max} 3461, 2963, 2928, 2873, 1698, 1455, 1380 cm^{-1}; ^1H NMR and ^{13}C NMR data, see Tables 1 and 2; ESIMS *m*/*z* 361 $[M+Na]^+$; HRESIMS *m*/*z* 361.2353 $[M+Na]^+$ (calcd for $C_{20}H_{34}O_4Na$, 361.2355).

Crassarine B (**2**): colorless oil; $[\alpha]^{24}_{D}$ –13 (c 0.11, $CHCl_3$); IR (KBr) ν_{max} 3288, 2957, 2925, 2855, 1732, 1698, 1453, 1372, 1237 cm^{-1}; ^1H NMR and ^{13}C NMR data, Tables 1 and 2; ESIMS *m*/*z* 403 $[M+Na]^+$; HRESIMS *m*/*z* 403.2463 $[M+Na]^+$ (calcd for $C_{22}H_{36}O_5Na$, 403.2460).

Crassarine C (**3**): colorless oil; $[\alpha]^{24}_{D}$ –45 (c 0.10, $CHCl_3$); IR (KBr) ν_{max} 3483, 2955, 2925, 2855, 1725, 1698, 1455, 1375, 1171 cm^{-1}; ^1H NMR and ^{13}C NMR data, Tables 1 and 2; ESIMS *m*/*z* 389 $[M+Na]^+$; HRESIMS *m*/*z* 389.2302 $[M+Na]^+$ (calcd for $C_{21}H_{34}O_5Na$, 389.2304).

Crassarine D (**4**): colorless oil; $[\alpha]^{24}_{D}$ –48 (c 0.34, $CHCl_3$); IR (KBr) ν_{max} 3386, 2955, 2925, 2855, 1716, 1458, 1268, 1036 cm^{-1}; ^1H NMR and ^{13}C NMR data, Tables 1 and 3; ESIMS *m*/*z* 361 $[M+Na]^+$; HRESIMS *m*/*z* 361.2354 $[M+Na]^+$ (calcd for $C_{20}H_{34}O_4Na$, 361.2355).

Crassarine E (**5**): colorless oil; $[\alpha]^{24}_{D}$ –27 (c 0.23, $CHCl_3$); IR (KBr) ν_{max} 3453, 2957, 2925, 2855, 1713, 1458, 1261, 1044 cm^{-1}; ^1H NMR and ^{13}C NMR data, Tables 1 and 3; ESIMS *m*/*z* 361 $[M+Na]^+$; HRESIMS *m*/*z* 361.2357 $[M+Na]^+$ (calcd for $C_{20}H_{34}O_4Na$, 361.2355).

Crassarine F (**6**): colorless oil; $[\alpha]^{24}_{D}$ –63 (c 0.18, $CHCl_3$); IR (KBr) ν_{max} 3300, 2960, 2926, 2857, 1668, 1458, 1380, 1255, 1036 cm^{-1}; ^1H NMR and ^{13}C NMR data, Tables 1 and 3; ESIMS *m*/*z* 327 $[M+Na]^+$; HRESIMS *m*/*z* 327.2302 $[M+Na]^+$ (calcd for $C_{20}H_{32}O_2Na$, 327.2300).

Crassarine G (**7**): colorless oil; $[\alpha]^{24}_{D}$ –41 (c 0.73, $CHCl_3$); IR (KBr) ν_{max} 3434, 2959, 2928, 2872, 1671, 1459, 1383, 1011 cm^{-1}; ^1H NMR and ^{13}C NMR data, Tables 1 and 3; ESIMS *m*/*z* 327 $[M+Na]^+$; HRESIMS *m*/*z* 327.2302 $[M+Na]^+$ (calcd for $C_{20}H_{32}O_2Na$, 327.2300).

Crassarine H (**8**): colorless oil; $[\alpha]^{24}_{D}$ –12 (c 0.22, $CHCl_3$); IR (KBr) ν_{max} 2955, 2922, 2855, 1458, 1380 cm^{-1}; ^1H NMR and ^{13}C NMR data, Tables 1 and 2; ESIMS *m*/*z* 325 $[M+Na]^+$; HRESIMS *m*/*z* 325.2145 $[M+Na]^+$ (calcd for $C_{20}H_{30}O_2Na$, 325.2143).

*3.4. Acetylation of **1***

To a stirring solution of compound **1** (0.1 mg) in pyridine (1 mL) was successively added excess acetic acid anhydrous (0.2 mL). After the mixture was stirred over night at rt, H_2O (0.3 mL) was added, and this mixture was subsequently extracted with EtOAc (5 × 6 mL). The combined EtOAc extract was successively washed with saturated aqueous $NaHCO_3$ and brine. The organic layer was dried over anhydrous Na_2SO_4 and concentrated to give a residue, which was chromatographed on silica gel with *n*-hexane-EtOAc (2:1) as eluent to afford **1a** (0.1 mg) which showed a $[M+Na]^+$ peak at *m*/*z* 403 in ESIMS spectrum. Selected ^1H NMR ($CDCl_3$, 300 MHz) spectrum of **1a**: δ 5.89 (1H, d, *J* = 15.9 Hz, H-2 or H-3), 5.77 (1H, d, *J* = 15.9 Hz, H-2 or H-3), 4.83 (1H, br d, *J* = 9.9 Hz, H-11), 2.95 (1H, d, *J* = 15.0 Hz, H-5a), 2.46□2.56 (2H, m, H-5b, H-7a), 2.08 (3H, s, $OCOCH_3$), 1.37 (3H, s, H_3-18), 1.20 (3H, s, H_3-18), 0.85□0.89 (9H, overlapped, H_3-19, H_3-16, and H_3-17).

*3.5. Preparation of (S)- and (R)-MTPA Esters of **6***

To a solution of **6** (0.5 mg) in pyridine (0.4 mL) was added (*R*)-MTPA chloride (25 μL), and the mixture was allowed to stand for 3 h at room temperature. The reaction was quenched by the addition

of 1.0 mL of H_2O, and the mixture was subsequently extracted with EtOAc (3 × 1.0 mL). The EtOAc layers were combined, dried over anhydrous $MgSO_4$, and evaporated. The residue was subjected to short silica gel column chromatography using *n*-hexane−EtOAc (8:1) to yield the (*S*)-MTPA ester, **6a** (0.3 mg). The same procedure was used to prepare the (*R*)-MTPA ester, **6b** (0.4 mg from 0.5 mg of **1**), with (*S*)-MTPA chloride. Selected ^{1}H NMR ($CDCl_3$, 300 MHz) of **6a**: δ 7.38−7.50 (5H, m, Ph), 6.14 (1H, d, *J* = 11.4 Hz, H-2), 6.00 (1H, d, *J* = 11.4 Hz, H-3), 5.61–5.71 (2H, overlapped, H-7 and H-9), 3.69 (1H, d, *J* = 12.0 Hz, H-11), 3.56 (3H, s, OMe), 1.80 (3H, s, H_3-18), 1.39 (3H, s, H_3-19), 1.10 (3H, s, H_3-20), 1.07 (3H, d, *J* = 6.9 Hz, H_3-16 or H_3-17), 1.03 (3H, d, *J* = 6.9 Hz, H_3-16 or H_3-17); selected ^{1}H NMR ($CDCl_3$, 300 MHz) of **6b**: δ 7.38−7.50 (5H, m, Ph), 6.13 (1H, d, *J* = 11.4 Hz, H-2), 5.98 (1H, d, *J* = 11.4 Hz, H-3), 5.67–5.78 (2H, overlapped, H-7 and H-9), 3.70 (1H, d, *J* = 10.2 Hz, H-11), 3.52 (3H, s, OMe) 1.78 (3H, s, H_3-18), 1.22 (3H, s, H_3-19), 1.13 (3H, s, H_3-20), 1.12 (3H, d, *J* = 6.9 Hz, H_3-16 or H_3-17), 1.03 (3H, d, *J* = 6.7 Hz, H_3-16 or H_3-17).

3.6. Cytotoxicity Testing

Cell lines were purchased from the American Type Culture Collection (ATCC). Cytotoxicity assays were performed using the MTT [3-(4,5-dimethylthiazole-2-yl)-2,5-diphenyltetrazolium bromide] colorimetric method [19].

3.7. In Vitro Anti-inflammatory Assay

Macrophage (RAW264.7) cell line was purchased from ATCC. In vitro anti-inflammatory activities of tested compounds were measured by examining the inhibition of lipopolysaccharide (LPS) induced upregulation of iNOS and COX-2 proteins in macrophage cells using western blotting analysis [20,21].

4. Conclusions

Cembranoids with a 1,12-oxa-bridged THF ring, such as compounds **1**–**3**, are rare in natural products. Incensole [22], incensole oxide [23], and incensole acetate [24] are the cembranoids of this class which were isolated from frankincense, the resin produced by the plant Boswellia carteri. It is also noteworthy that the formyloxyl cembranoid, such as **3**, and the 1,11-oxa-bridged tetrahydropyranocembranoids, such as **4** and **5**, were discovered for the fist time.

Acknowledgments

This work was supported by grants from the National Science Council of Taiwan (NSC98-2113-M-110-002-MY3) and Ministry of Education (98C031702) awarded to J.-H. S.

References

1. Blunt, J.W.; Copp, B.R.; Munro, M.H.G.; Northcote, P.T.; Prinsep, M.R. Marine natural products. *Nat. Prod. Rep.* **2011**, *28*, 196–268.

2. Su, J.-H.; Ahmed, A.F.; Sung, P.-J.; Chao, C.-H.; Kuo, Y.-H.; Sheu, J.-H. Manaarenolides A–I, diterpenoids from the soft coral *Sinularia manaarensis*. *J. Nat. Prod.* **2006**, *69*, 1134–1139.
3. Chao, C.-H.; Wen, Z.-H.; Wu, Y.-C.; Yeh, H.-C.; Sheu, J.-H. Cytotoxic and anti-inflammatory cembranoids from the soft coral *Lobophytum crassum*. *J. Nat. Prod.* **2008**, *71*, 1819–1824.
4. Lu, Y.; Huang, C.-Y.; Lin, Y.-F.; Wen, Z.-H.; Su, J.-H.; Kuo, Y.-H.; Chiang, M.Y.; Sheu, J.-H. Anti-inflammatory cembranoids from the soft corals *Sinularia querciformis* and *Sinularia granosa*. *J. Nat. Prod.* **2008**, *71*, 1754–1759.
5. Tseng, Y.-J.; Ahmed, A. F.; Dai, C.-F.; Chiang, M. Y.; Sheu, J.-H. Sinulochmodins A−C, three novel terpenoids from the soft coral *Sinularia lochmodes*. *Org. Lett.*, 2005, **7**, 3813–3816.
6. Ahmed, A. F.; Su, J.-H.; Kuo, Y.-H.; Sheu, J.-H. Scabrolides E−G, three new norditerpenoids from the soft coral *Sinularia scabra*. *J. Nat. Prod*., 2004, **67**, 2079–2082.
7. Ahmed, A. F.; Shiue, R.-T.; Wang, G.-H.; Dai, C.-F.; Kuo, Y.-H.; Sheu, J.-H. Five novel norcembranoids from *Sinularia leptoclados* and *S. parva*. *Tetrahedron,* 2003, **59**, 7337–7344.
8. Sheu, J.-H.; Ahmed, A. F.; Shiue, R.-T.; Dai, C.-F.; Kuo, Y.-H. Scabrolides A−D, four new norditerpenoids isolated from the soft coral *Sinularia scabra*. *J. Nat. Prod*., 2002, **65**, 1904–1908.
9. Radhika, P.; Rao, P. R.; Archana, J.; Rao, N. K. Anti-inflammatory activity of a new sphingosine derivative and cembrenoid diterpene (lobohedleolide) isolated from marine soft corals of *Sinularia crassa* Tixier-Durivault and *Lobophytum* species of the Andaman and Nicobar Islands. *Biol. Pharm. Bull*., 2005, **28**, 1311–1313.
10. Anjaneyulu, V.; Radhika, P. Two new sphingosine derivatives from *Sinularia crassa* Tixier-Durivault of the Andaman and Nicobar Islands. *Indian J. Chem.*, 1999, **38B**, 457–460.
11. Radhika, P.; Cabeza, M.; Bratoeff, E.; García,G. 5α-Reductase inhibition activity of steroids isolated from marine soft corals. *Steroids*, 2004, **69**, 439–444.
12. König, G.M.; Wright, A.D. New cembranoid diterpenes from the soft coral *Sarcophyton ehrenbergi*. *J. Nat. Prod.* **1998**, *61*, 494–496.
13. Demarco, P. V.; Farkas, E.; Doddrell, D.; Mylari, B. L.; Wenkert, E. Pyridine-induced solvent shifts in the nuclear magnetic resonance spectra of hydroxylic compounds. *J. Am. Chem. Soc*., 1968, **90**, 5480–5486.
14. Ahmed, A. F.; Wu, M.-H.; Wang, G.-H.; Wu, Y.-C.; Sheu, J.-H. Eunicellin-based diterpenoids, australins A−D, isolated from the soft coral *Cladiella australis*. *J. Nat. Prod*., 2005, **68**, 1051–1055.
15. Ahmed, A.F.; Wen, Z.-H.; Su, J.-H.; Hsieh, Y.-T.; Wu, Y.-C.; Hu, W.-P.; Sheu, J.-H. Oxygenated cembranoids from a Formosan soft coral *Sinularia gibberosa*. *J. Nat. Prod.* **2008**, *71*, 179–185.
16. Ohtani, I.; Kusumi, T.; Kashman, Y.; Kakisawa, H. High-field FT NMR application of Mosher's method. The absolute configurations of marine terpenoids. *J. Am. Chem. Soc*., 1991, **113**, 4092–4096.
17. Randazzo, A.; Bifulco, G.; Giannini, C.; Bucci, M.; Debitus, C.; Cirino, G.; Gomez-Paloma, L. Halipeptins A and B: two novel potent anti-inflammatory cyclic depsipeptides from the vanuatu marine sponge *Haliclona species*. *J. Am. Chem. Soc*., 2001, **123**, 10870–10876.
18. Williams, D.; Andersen, R. J. Cembrane and pseudopterane diterpenes from the soft coral *Gersemia rubiformis*. *J. Org. Chem*., 1987, **52**, 332–335.

19. Alley, M.C.; Scudiero, D.A.; Monks, A.; Hursey, M.L.; Czerwinski, M.J.; Fine, D.L.; Abbott, B.J.; Mayo, J.G.; Shoemaker, R.H.; Boyd, M.R. Feasibility of drug screening with panels of human tumor cell lines using a microculture tetrazolium assay. *Cancer Res.* **1988**, *48*, 589–601.
20. Jean, Y.-H.; Chen, W.-F.; Sung, C.-S.; Duh, C.-Y.; Huang, S.-Y.; Lin, C.-S.; Tai, M.-H.; Tzeng, S.-F.; Wen, Z.-H. Capnellene, a natural marine compound derived from soft coral, attenuates chronic constriction injury-induced neuropathic pain in rats. *Br. J. Pharmacol.* **2009**, *158*, 713–725.
21. Jean, Y.-H.; Chen, W.-F.; Duh, C.-Y.; Huang, S.-Y.; Hsu, C.-H.; Lin, C.-S.; Sung, C.-S.; Chen, I.-M.; Wen, Z.-H. Inducible nitric oxide synthase and cyclooxygenase-2 participate in anti-inflammatory and analgesic effects of the natural marine compound lemnalol from Formosan soft coral *Lemnalia cervicorni*. *Eur. J. Pharmacol.* **2008**, *578*, 323–331.
22. Corsano, S.; Nicoletti, R. The structure of incensole. *Tetrahedron*, 1967, **23**, 1977–1984.
23. Nicoletti, R.; Forcellese, M. L. The structure of incensole-oxide. *Tetrahedron*, 1968, **24**, 6519–6525.
24. Boscarelli, A.; Giglio, E.; Quagliata, C. Structure and conformation of incensole oxide. *Acta. Cryst.*, 1981, **B37**, 744–746.

Samples Availability: Not available.